MAJOR ARTICLE

# Pathogenesis of *Aspergillus fumigatus* and the Kinetics of Galactomannan in an In Vitro Model of Early Invasive Pulmonary Aspergillosis: Implications for Antifungal Therapy

**William W. Hope,[1] Michael J. Kruhlak,[2] Caron A. Lyman,[1] Ruta Petraitiene,[1,4] Vidmantas Petraitis,[1,4] Andrea Francesconi,[1] Miki Kasai,[1] Diana Mickiene,[1,4] Tin Sein,[1,4] Joanne Peter,[1] Amy M. Kelaher,[1] Johanna E. Hughes,[1] Margaret P. Cotton,[1] Catherine J. Cotten,[1] John Bacher,[3] Sanjay Tripathi,[6] Louis Bermudez,[6] Timothy K. Maugel,[5] Patricia M. Zerfas,[3] John R. Wingard,[7] George L. Drusano,[8] and Thomas J. Walsh[1]**

[1]Immunocompromised Host Section, Pediatric Oncology Branch, and [2]Experimental Immunology Branch, National Cancer Institute, and [3]Veterinary Resources Program, Office of Research Services, National Institutes of Health, Bethesda, [4]SAIC-Frederick, Inc., Frederick, and [5]Department of Biology, University of Maryland, College Park, Maryland; [6]Department of Biomedical Sciences, College of Veterinary Medicine, Oregon State University, Corvallis; [7]University of Florida College of Medicine, Gainesville; [8]Emerging Infectious Diseases Unit, Ordway Research Institute, Albany, New York

***Background.*** Little is known about the pathogenesis of invasive pulmonary aspergillosis and the relationship between the kinetics of diagnostic markers and the outcome of antifungal therapy.

***Methods.*** An in vitro model of the human alveolus, consisting of a bilayer of human alveolar epithelial and endothelial cells, was developed. An *Aspergillus fumigatus* strain expressing green fluorescent protein was used. Invasion of the cell bilayer was studied using confocal and electron microscopy. The kinetics of culture, polymerase chain reaction, and galactomannan were determined. Galactomannan was used to measure the antifungal effect of macrophages and amphotericin B. A mathematical model was developed, and results were bridged to humans.

***Results.*** *A. fumigatus* penetrated the cellular bilayer 14–16 h after inoculation. Galactomannan levels were inextricably tied to fungal invasion and were a robust measure of the antifungal effect of macrophages and amphotericin B. Neither amphotericin nor macrophages alone was able to suppress the growth of *A. fumigatus;* rather, the combination was required. Monte Carlo simulations showed that human dosages of amphotericin B of at least 0.6 mg/kg were required to achieve adequate drug exposure.

***Conclusions.*** This model provides a strategy by which relationships among pathogenesis, immunological effectors, and antifungal drug therapy for invasive pulmonary aspergillosis may be further understood.

*Aspergillus fumigatus* is an opportunistic pathogen that causes life-threatening infections in a wide range of immunocompromised hosts and has an overall mortality rate of ~50% [1–3]. There remains an urgent requirement to improve the therapeutic outcome of invasive aspergillosis.

Little is known, however, about the relationship between the earliest events in the invasion of *A. fumigatus,* the kinetics of diagnostic markers, and the effect of immunological effectors and antifungal agents. The *Aspergillus* cell-wall antigen, galactomannan, has been increasingly used as a diagnostic marker for invasive pulmonary aspergillosis (IPA) [4, 5], but there is a relative paucity of data describing the relationship among levels of galactomannan, the pathogenesis of IPA, and its role in monitoring the therapeutic response. Although there has been an increased understanding of the pharmacodynamic relationships of antifungal agents against *Candida albicans* [6, 7], there remains only a rudi-

Received 22 May 2006; accepted 27 July 2006; electronically published 21 December 2006.

Potential conflicts of interest: none reported.

Financial support: National Cancer Institute, National Institutes of Health (Intramural Research Program); National Marrow Donor Program (Amy Strelzer Manasevit Fellowship to W.W.H.).

Reprints or correspondence: Dr. Thomas J. Walsh, Immunocompromised Host Section, Bldg. 10-CRC, Rm. 1-5750, Pediatric Oncology Branch, National Cancer Institute, National Institutes of Health, Bethesda, MD 20892 (walsht@mail.nih.gov).

**The Journal of Infectious Diseases 2007; 195:455–66**



0022-1899/2007/19503-0021$15.00

mentary understanding of concentration-effect relationships for *Aspergillus.*

To address these issues, we developed and validated an in vitro model of the human alveolus to study the relationship among the pathogenesis of early IPA, the kinetics of diagnostic markers, and the outcome of antifungal therapy. We used galactomannan to quantify fungal growth and the antifungal effect induced by macrophages and amphotericin B, both alone and in combination. A population mathematical model was developed, and Monte Carlo simulation was used to further explore the clinical implications of the experimental results.

## MATERIALS AND METHODS

***Construction of the cell bilayer and validation of the in vitro model.*** Human pulmonary artery endothelial cells (HPAECs) were purchased from Cambrex Bio Science. Human alveolar epithelial (A549) cells were purchased from American Type Culture Collection. HPAECs were only used in passages 6 and 7. HPAECs were grown in endothelial medium (basal medium [EBM-2] supplemented with ascorbic acid, heparin, hydrocortisone, human endothelial growth factor [EGF], 2% fetal bovine serum [FBS], vascular EGF, human fibroblast growth factor–B, and R3–insulin-like growth factor–1), to form EGM-2. Amphotericin B and gentamicin, which are ordinarily components of EGM-2, were not included. Cells were grown to near-confluence in humidified 5% $CO_2$ at 37°C. A549 cells were used in passages 79–86 and were grown in EBM-2 supplemented with 10% FBS only (Gemini Bioproducts).

A bilayer was constructed using 6.5-mm-diameter Transwell Clear membranes with 3-$\mu$m pores (Corning). A total of $1 \times 10^5$ HPAECs suspended in 100 $\mu$L was placed onto the undersurface of the membrane and incubated for at least 2 h. Membranes were subsequently placed right side up in a 24-well tissue culture plate that contained 600 $\mu$L of endothelial medium, and 100 $\mu$L of EGM-2 medium was added to the upper chamber. The membranes were incubated in 5% $CO_2$ for 24 h at 37°C. Subsequently, $5 \times 10^4$ A549 cells suspended in 100 $\mu$L of EBM-2 supplemented with 10% FBS were seeded on the top surface of the membrane. The respective media were changed daily. All experiments were performed on day 5 after inoculation of A549 cells and were performed in different media. For HPAECs, EBM-2 was only supplemented with 2% FBS; for the A549 cells, EBM-2 only was used.

Cellular confluence was assessed by placing 100 $\mu$L of 1% dextran blue (Sigma) in the alveolar compartment and 600 $\mu$L of PBS warmed to 37°C in the endothelial compartment and incubating for 2 h. The concentration of dextran blue in the endothelial compartment was determined spectrophotometrically. Transmembrane resistance was assessed using the Millipore meter (Millipore) as described elsewhere [8].

Elutriated human monocytes were obtained from healthy donors. Cells were grown in RPMI with L-glutamine (Cellgro) supplemented with 10% FBS. Macrophage colony-stimulating factor (Cetus) was added to a final concentration of 20 $\mu$g/L. The cells were incubated in 5% $CO_2$ for 48 h at 37°C before harvesting. Three effector:target (E:T) ratios were studied: 1:1, 10:1, and 100:1. Cell viability was assessed via the exclusion of trypan blue (Cambrex Biosciences).

***Organism.*** An *A. fumigatus* transformant expressing green fluorescent protein was a gift from Professor Margo Moore (Simon Fraser University, Burnaby, British Columbia, Canada) [9, 10]. Fresh conidial suspensions were prepared before each experiment. The inoculum was verified by quantitative cultures. The MICs were 0.4, 0.4, and 0.5 mg/L according to a Clinical and Laboratory Standards Institute M38 A methodology [11] on 3 separate occasions; a MIC of 0.5 mg/L was used.

***Confocal and electron microscopy.*** For confocal microscopy, membranes were fixed with 4% paraformaldehyde (Electron Microscopy Sciences) and stained with 4′,6′-diamidino-2-phenylindole (Roche Applied Science). Imaging was performed with a Zeiss LSM 510 META confocal microscope (Carl Zeiss Microimaging) equipped with a 40× Apochromat (numerical aperture, 1.2) objective lens. Image *z*-stacks with 0.22-$\mu$m *x-y* pixel size and 1.0-$\mu$m optical slice thickness were collected. For electron microscopy, membranes were fixed in 2% glutaraldehyde in 0.1 mol/L cacodylate buffer and subsequently processed. Transmission electron microscopy was performed using a Philips 410 electron microscope (FEI) at 80 kV, and scanning images were obtained using a Hitachi S-4700 FESEM device (Hitachi High Technologies America).

***Diagnostic markers of IPA from the membrane and supernatant.*** Quantitative cultures from the membranes were determined after pretreatment with chaotropic beads (Qbiogene/MP Biomedical). DNA was extracted using MagNA Pure LC using MagNA Pure LC DNA Isolation Kit III (Roche Diagnostics, Roche Applied Science) after enzymatic disruption and treatment with chaotropic beads. Polymerase chain reaction (PCR) was performed using a real-time assay with primers directed toward the ITS1-5.8S-ITS2 region of the rRNA complex, as described elsewhere [12]. A control for DNA extraction was achieved by quantifying human $\beta$-globin DNA (Roche Applied Science). Levels of galactomannan in cell-culture medium, rabbit serum, and rabbit bronchoalveolar lavage (BAL) fluid were determined using ELISA (Bio-Rad Laboratories) [13].

***Drug, drug measurement, and pharmacokinetics.*** Amphotericin B (Pharma-Tek) was added to EBM-2 supplemented with 2% FCS. Drug concentrations were determined using high-performance liquid chromatography as described elsewhere, with minor modifications [14]. A volume of 150 $\mu$L was submitted to analysis. The pharmacokinetics of amphotericin B in the in vitro model was studied in the alveolar and en-

dothelial compartment after initial concentrations of 0.1, 0.5, 1, and 2 mg/L, with sampling at 1, 3, 6, 14, 18, 24, and 30 h.

***Neutropenic rabbit model of invasive pulmonary aspergillosis.*** A neutropenic rabbit model of invasive pulmonary aspergillosis, described elsewhere [15], was used. *A. fumigatus* strain NIH 4215 was used. Rabbits were serially killed at 4, 8, 12, 16, 20, 24, and 30 h after inoculation. A BAL was performed using 20 mL of 0.9% saline, and the fluid was centrifuged at 13,000 *g* for 10 min and the supernatant submitted for galactomannan estimation.

***Data analysis, mathematical modeling, and Monte Carlo simulation.*** Experimental data from the alveolar and endothelial compartments were comodeled with a population methodology using the Big NPAG program [16]. These data included (1) the pharmacokinetics of amphotericin B, (2) the effect of various dosages of amphotericin B on the time course of galactomannan, (3) the effect of macrophages in their various E:T ratios on the time course of galactomannan, and (4) the combined effect of amphotericin B and macrophages on the time course of galactomannan. The structural model is contained in the appendix. The data were weighted by the inverse of the observed variance.

The mean parameter values obtained from the population analysis were used to define the concentration of amphotericin B administered to the endothelial compartment, which resulted in suppression of the galactomannan levels in the alveolar and endothelial compartments. To further explore the therapeutic implications of these experimental results, the data were bridged to humans. The results of a study by Nath et al. [17], which described the population pharmacokinetics of amphotericin B in children, were applied to a 70-kg human. A 9999-subject simulation was performed. The proportion of simulated patients who received 0.3, 0.6, and 1 mg/kg and attained or exceeded a level of drug exposure predicted to suppress the growth of *A. fumigatus* was defined.

## RESULTS

***In vitro model of the alveolus.*** A schematic representation of the in vitro model is shown in figure 1*A*. The integrity of the cellular bilayer was evident at an ultrastructural level (figure 1*B*).

Confluence of the cellular bilayer was evident 4 days after seeding of the A549 human type II pneumocytes. This was most readily apparent after a sustained difference in the levels of medium used for the alveolar and endothelial cells (figure 1). The transmembrane resistance of the cellular bilayer was $555 \pm 12.25\ \Omega/cm^2$ (resistance across the membrane alone, $360\ \Omega/cm^2$). There was negligible translocation of dextran blue across the bilayer throughout the experimental period, in both infected and drug-exposed systems.

***Organisms, infection of the cellular bilayer with* A. fumigatus*, and the microscopic and ultrastructural features of the in vitro model.*** After the inoculation of conidia into the alveolar compartment, type II pneumocytes ingested conidia (fig-

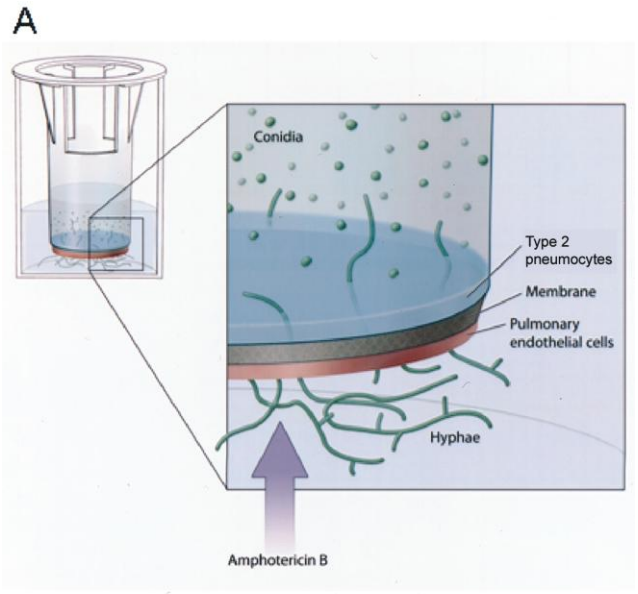


**Figure 1.** In vitro model of the human alveolus. *A,* Schematic representation of the model. Confluence of the cellular bilayer was associated with the development of transmembrane electrical resistance, prevention of the translocation of dextran blue, and a sustained difference in the level of cell culture medium within the respective compartments. *B,* Cellular bilayer composed of A549 cells (A), human pulmonary artery endothelial cells (E), and the membrane (M) with pores (P). Scale bar, 10 $\mu$m; magnification, $\times$2120.

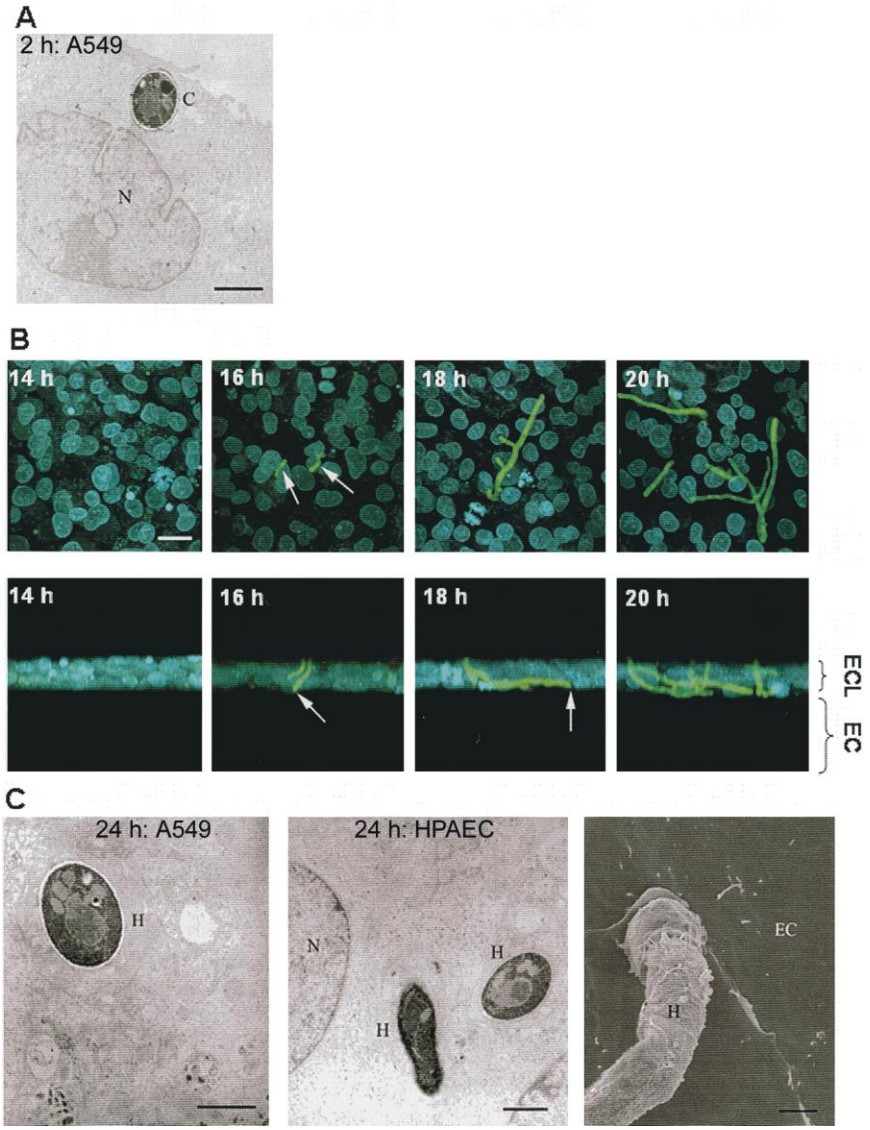


**Figure 2.** Microscopic and ultrastructural features of the in vitro model and invasion of the green fluorescent protein (GFP) modified *Aspergillus fumigatus*. *A,* Conidia (C) are ingested by A549 cells 2 h after inoculation. *B,* Confocal images of the endothelial cell layer (ECL) and the underlying endothelial compartment (EC) taken 14, 16, 18, and 20 h after inoculation. The second row of images have been rotated to provide a cross-section of the cellular bilayer. Arrows show hyphae and the extending hyphal tips. Scale bar, 10 $\mu$m. *C,* hyphae (H) invading directly through alveolar and the EC 24 h after inoculation. N, nucleus. Scale bar, 2 $\mu$m. HPAEC, human pulmonary artery endothelial cells.

ure 2*A*). Confocal microscopy showed that hyphae emerged from the endothelial cell layer into the endothelial compartment ~14–16 h after inoculation (figure 2*B*). With the passage of time, there was progressive hyphal extension through the endothelial cell layer and into the endothelial compartment. The transmission and scanning electron images show that the invasion of *Aspergillus* assumed a direct intracellular path through both alveolar and endothelial cells (figure 2*C–E*).

***Time course of conventional culture, quantitative* Aspergillus *PCR, galactomannan, and the inoculum-effect relationship.*** Quantitative cultures from the membrane after inoculation with $10^3$, $10^4$, and $10^5$ conidia did not change throughout the experimental period and therefore did not reflect the progressive growth and invasion of *Aspergillus* through the cellular bilayer that was evident at a microscopic and ultrastructural level (figure 3*A*). By contrast, the PCR signal from the membranes reflected a logarithmic increase in DNA content (figure 3*B*). Cultures from the alveolar compartment were positive immediately after inoculation, but subsequently only intermittently so, with no clear relationship to the inoculum (data not shown). The cultures from the endothelial compartment remained sterile throughout the course of the experiment, even when there was clear evidence of hyphal growth within this compartment (data not shown). Compared with galactoman-

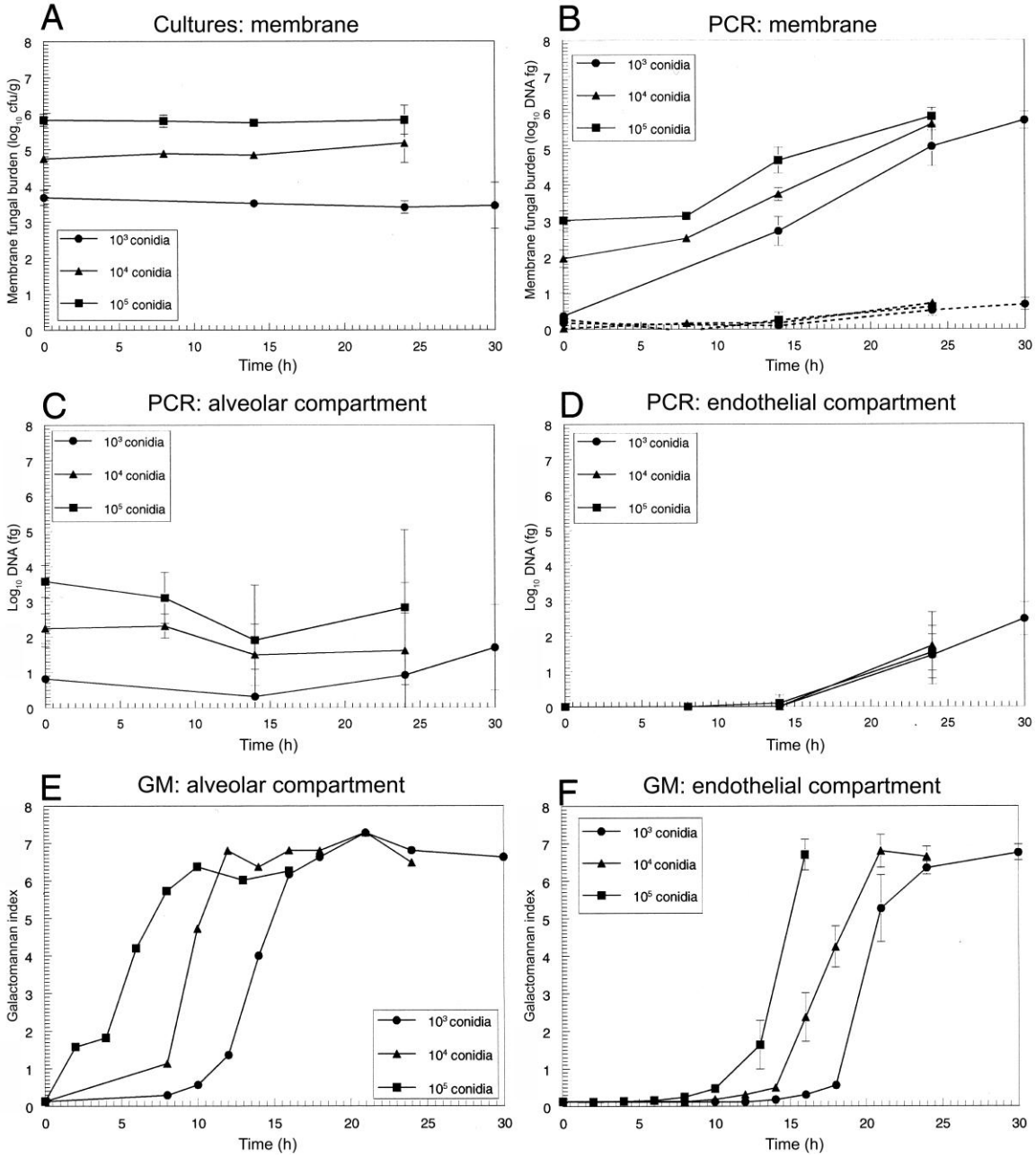


**Figure 3.** Kinetics of diagnostic modalities for invasive aspergillosis after inoculation with $10^3$, $10^4$, and $10^5$ conidia in the in vitro model. *A,* Time course of quantitative cultures from the polyester membrane. *B,* Time course of polymerase chain reaction (PCR) signal from the polyester membrane. Broken lines show the $\beta$-globin PCR signal. *C,* PCR signal from the supernatant within the alveolar compartment. *D,* PCR signal from the supernatant within the endothelial compartment. *E,* Galactomannan (GM) levels from the alveolar compartment. *F,* Galactomannan levels from the endothelial compartment.

nan levels, quantitative PCR was less reflective of the growth and dynamics of *Aspergillus*, particularly within the alveolar compartment.

Galactomannan levels were highly reproducible, and the effect of the 3 inocula could be distinguished in both of the compartments of the model (figure 3*E* and 3*F*). Most important, however, the kinetic profile of galactomannan was correlated with critical cellular events in the invasion of *Aspergillus* as determined by confocal microscopy. Figure 4 demonstrates that the levels of galactomannan began to increase in the endothelial compartment 14–16 h after inoculation, which coincided with the penetration of hyphae through the endothelial cell layer and into the endothelial compartment (figure 2*B*). Therefore, galactomannan was subsequently used to measure

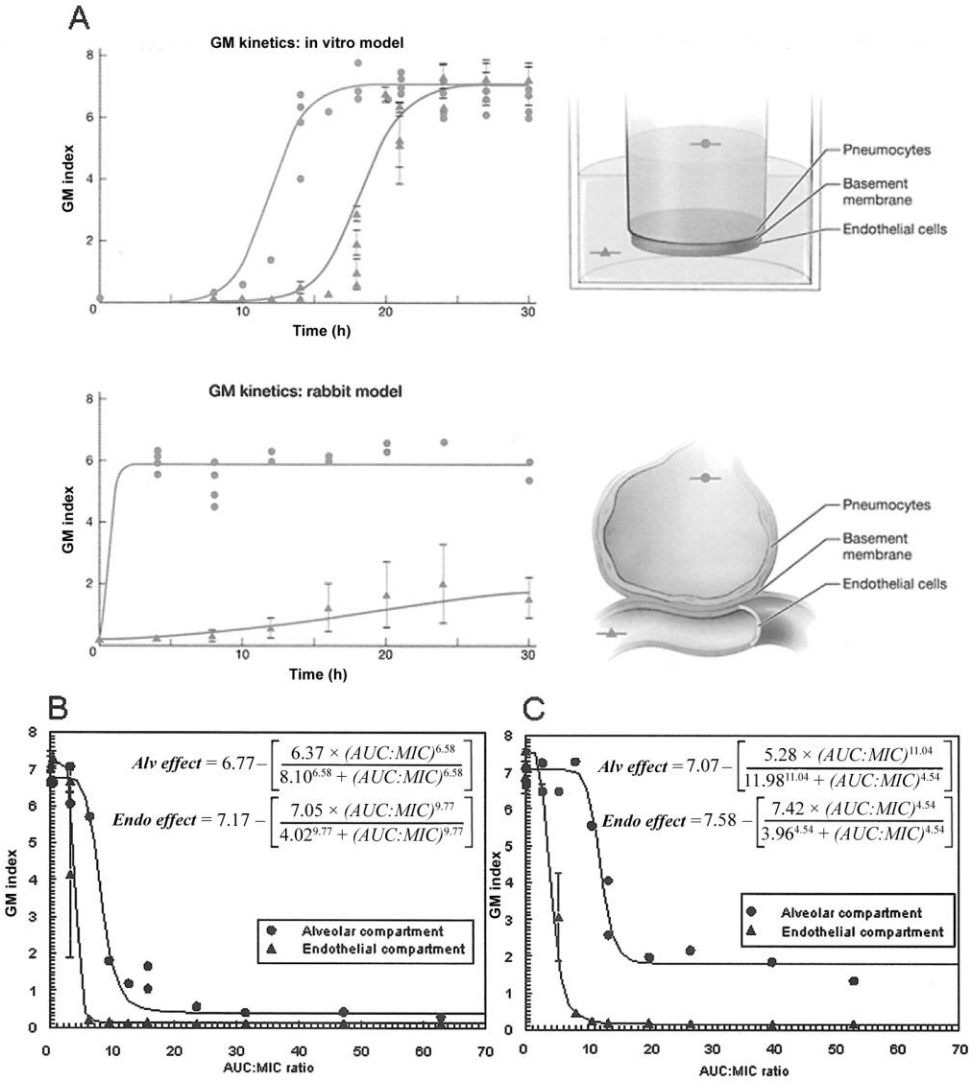


**Figure 4.** Validation of the in vitro model against a neutropenic rabbit model of invasive pulmonary aspergillosis and the further development of a model in which the administration of amphotericin B is delayed by 6 h. *A,* Time course of galactomannan (GM) in the alveolar and endothelial in the in vitro model, compared with the rabbit model, showing discordant kinetics of GM between the alveolar and endothelial compartments. There was a delay in the appearance of GM within the endothelial compartment (serum in rabbits) that corresponded to the time taken for conidial germination and invasion of the alveolar-capillary barrier. *B,* Exposure-response relationships when there was no delay in the administration of amphotericin B to the endothelial compartment. *C,* Exposure-response relationship after a 6-h delay in drug administration. A delay in the administration of amphotericin B was detrimental, given the incomplete suppression of growth within the alveolar compartment. AUC, area under the curve.

unrestrained fungal growth and the antifungal effect of macrophages and amphotericin B.

***Discordant kinetics of galactomannan in the alveolar and endothelial compartments: in vitro–in vivo correlations.*** The time course of galactomannan levels in BAL and serum specimens obtained from neutropenic rabbits with IPA was compared with that observed in the in vitro model. Figure 4*A* shows that the levels of galactomannan in the endovascular compartment (serum from rabbits) and the alveolar compartment (BAL fluid from rabbits) were discordant. The delay between the appearance of galactomannan in BAL and serum likely reflected the time taken for advancing hyphae to traverse the alveolar-capillary barrier.

***Persistence of* A. fumigatus *after a delay in the administration of amphotericin B.*** The effect of (1) no delay and (2) a 6-h delay in the administration of amphotericin B into the endothelial compartment on the levels of galactomannan in the alveolar and endothelial compartments was explored (figure 4*B* and 4*C*). In both models, the galactomannan levels were determined at a single time point 30 h after inoculation. To correct for the different durations of drug exposure in the 2 experiments (i.e., 30 and 24 h in the no-delay and 6-h-delay model,

respectively), the data were transformed from concentration response to the area under the curve (AUC):MIC response relationships. The mean pharmacokinetic parameter values in table 1 were used for this purpose.

These experiments revealed that it was not possible to administer enough drug to completely inhibit the production of galactomannan in the alveolar compartment after a 6-h delay in the administration of amphotericin B. By contrast, the exposure-response relationships in the endothelial compartment of the respective models were comparable. Because a delay in the introduction of drug was more clinically tenable, we chose to use this model in all subsequent experiments.

***Pharmacokinetics of amphotericin B.*** The concentrations of amphotericin B decreased in the endothelial compartment as the drug traversed the cell layer and emerged within the alveolar compartment (figure 5). The pharmacokinetic parameters are summarized in table 1.

***Time course of the effect of amphotericin B in the endothelial and alveolar compartment.*** The effect of an initial concentration of 0.25, 0.5, and 2.0 mg/L of amphotericin B administered to the endothelial compartment 6 h after inoculation was studied. These concentrations were chosen on the basis of the inhibitory sigmoid $E_{max}$ relationship shown in figure 4*C*. The kinetics of galactomannan were determined in both the alveolar and the endothelial compartment. None of the concentrations of amphotericin B could suppress the levels of galactomannan in the alveolar compartment (figure 6*A*). By contrast, amphotericin B exhibited striking efficiency in its ability to suppress growth in the endothelial compartment. An initial concentration of both 0.5 and 2.0 mg/L suppressed galactomannan levels in the endothelial compartment, and a concentration of 0.25 mg/L suppressed growth for the majority of the experimental period (figure 6*B*).

***Effect of adding monocyte-derived macrophages to the alveolar compartment.*** Human monocyte–derived macrophages were added to the alveolar compartment to study the antifungal effect of resident pulmonary alveolar macrophages. Only an E:T ratio of 100:1 had any demonstrable influence on the time course of galactomannan, and even then the effect was merely to retard rather than to suppress the growth of *Aspergillus* (figure 6*C* and 6*D*).

***Effect of adding monocyte-derived macrophages to the alveolar compartment and amphotericin B to the endothelial compartment.*** Because neither amphotericin B (when administered after a 6-h delay) nor monocyte-derived macrophages could suppress the growth of *Aspergillus,* the antifungal

**Table 1. Model parameters and their means, medians, and SDs.**

| Parameter, units | Mean | Median | SD |
|---|---|---|---|
| $k_{12}$, per h | 0.042 | 0.028 | 0.045 |
| $k_{21}$, per h | 10.666 | 8.225 | 5.281 |
| $k_{23}$, per h | 9.207 | 6.297 | 6.985 |
| $V_e$, L | $0.87 \times 10^{-3}$ | $0.67 \times 10^{-3}$ | $0.34 \times 10^{-3}$ |
| $V_a$, L | $0.58 \times 10^{-3}$ | $0.47 \times 10^{-3}$ | $0.29 \times 10^{-3}$ |
| $Kgmax_e$, GMI/h | 0.653 | 0.649 | 0.078 |
| $H_e$ | 6.205 | 1.298 | 7.51 |
| $C50_e$, mg/L | 1.375 | 0.468 | 1.616 |
| *POPMAX,* GMI | 7.059 | 7.193 | 0.167 |
| $Kgmax_a$, GMI/h | 0.777 | 0.759 | 0.076 |
| $H_a$ | 16.673 | 18.989 | 5.678 |
| $C50_a$, mg/L | 0.162 | 0.051 | 0.208 |
| Initial condition of the endothelial compartment, GMI | $0.46 \times 10^{-4}$ | $0.57 \times 10^{-4}$ | $0.22 \times 10^{-4}$ |
| Initial condition of the alveolar compartment, GMI | $0.67 \times 10^{-3}$ | $0.74 \times 10^{-3}$ | $0.23 \times 10^{-3}$ |
| $WBCkillmax_e$, GMI/h | 0.873 | 0.046 | 1.044 |
| $WBCkill50_e$, GMI | 3.308 | 2.101 | 2.966 |
| $WBCkillmax_a$, GMI/h | 0.27 | 0.023 | 0.46 |
| $WBCkill50_a$, GMI | 3.616 | 3.208 | 3.173 |

**NOTE.** Subscripts "e" and "a" denote the endothelial and alveolar compartments, respectively; $k_{12}$, $k_{21}$, and $k_{23}$ represent the first-order intercompartmental rate constants; *V* is the volume of the respective compartments; *Kgmax* is the maximum-growth-rate constant of *Aspergillus; H* is the sigmoidicity (slope) constant for the effect of amphotericin B on growth; *C*50 is the concentration of amphotericin B that is required to achieve a 50% reduction in growth; *POPMAX* is the maximum achievable galactomannan value; *WBCkillmax* is the maximum rate of kill effected by macrophages, and *WBCkil*50 is the galactomannan value at which the macrophage kill is half-maximal. GMI, galactomannan index.

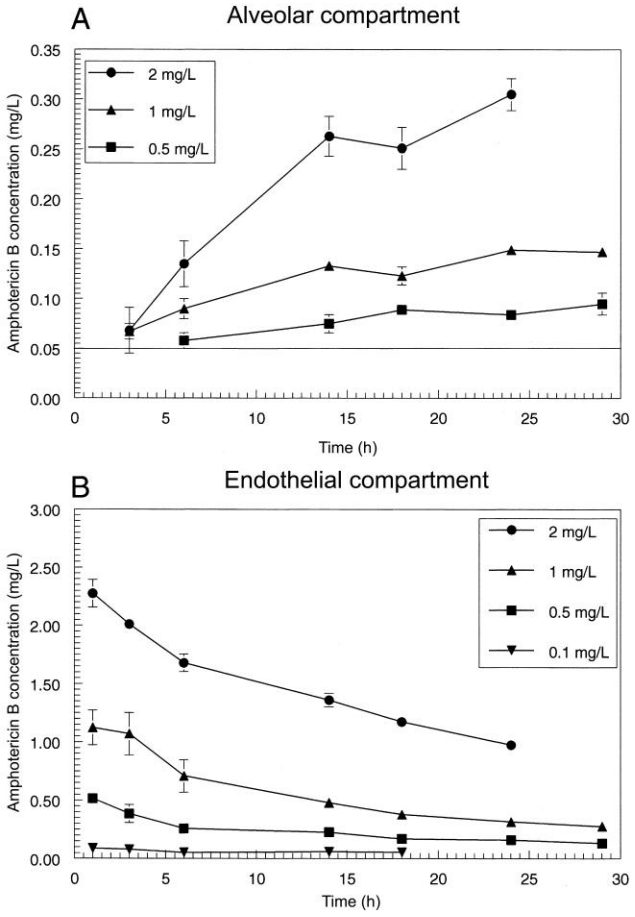


**Figure 5.** Pharmacokinetics of amphotericin B in the in vitro model. *A,* Amphotericin B emerging within the alveolar compartment after undergoing biexponential decay within the endothelial compartment *(B).*

effect of their combination was examined (figure 6*E* and 6*F*). In these experiments, macrophages at an E:T ratio of 100:1 were applied immediately before the inoculation of conidia into the alveolar compartment, and amphotericin B was administered at a concentration of 0.25 and 2.0 mg/L to the endothelial compartment 6 h later. The coadministration of macrophages with amphotericin B at an initial concentration of 0.25 mg/L resulted in the suppression of galactomannan in the endothelial compartment, which was not possible when this concentration of drug was used alone. Similarly, in the alveolar compartment, there was also suppression of galactomannan when concentrations of 0.25 and 2.0 mg/L amphotericin B were combined with macrophages. Thus, near-maximal suppression of the levels of galactomannan in both the alveolar and the endothelial compartment was possible, but only when amphotericin B was combined with macrophages at an E:T ratio of 100:1 (figure 6*E* and 6*F*).

***Mathematical model of the in vitro model and the bridging to humans using Monte Carlo simulation.*** The estimates of the mean and median values of the model parameters, along with their SDs, which were obtained from the combined mathematical model, are shown in table 1. The fit of the model to the data was excellent, with $r^2$ values >0.95 for the observed-versus-predicted values after the Bayesian step with highly acceptable measures of bias and precision. Model simulations were performed using the mean parameter values and a fixed E:T ratio of 100:1. An initial concentration of amphotericin B of 0.83 mg/L in the endothelial compartment, which produced an AUC of 11.05 and an AUC:MIC of 22.10, resulted in a galactomannan level <0.25 in the alveolar and endothelial compartments. An expectation of target attainment was determined for 9999 simulated human patients, each of whom received 0.3, 0.6, and 1 mg/kg of amphotericin B administered intravenously over the course of 2 h. The fraction of the simulated patients who attained or exceeded an AUC:MIC of 22.10 was determined for each of the amphotericin B MIC values between 0.25 and 4.0 mg/L. The overall target attainment rate for a dose of 0.3, 0.6, and 1.0 mg/kg of amphotericin B across the distribution of *A. fumigatus* MICs was 5.5%, 72.1%, and 94.7%, respectively.

## DISCUSSION

We adapted a cell bilayer model of the human alveolus, which has been used previously for the study of the translocation of *Mycobacterium tuberculosis* [8, 18], to further study early IPA. This approach provided the following advantages: (1) it enabled us to model clinically relevant tissue compartments and sampling sites; (2) it provided the ability to recapitulate human pathogenesis by allowing conidia to germinate in contact with alveolar epithelial cells, with a breaching of the endothelial cells by hyphae invading their basal aspect; (3) we were able to reflect on the antifungal effect of macrophages in various E:T ratios; and (4) we captured events that are operational at the very earliest point at which the pulmonary vasculature is breached.

The biological validity of the in vitro model was further explored by comparing it with an established neutropenic rabbit model of IPA. In addition to the architecture of the in vitro model, we attempted to recapitulate alveolar physiology in a number of potentially important ways. The endothelial compartment contained FBS, thereby simulating the protein content of blood and enabling the binding of drugs to protein that is observed in clinical and in vivo settings. Similarly, no FBS was added to the alveolar compartment, because the alveolus is usually devoid of albumin. In addition to adding macrophages to the alveolar compartment to simulate innate pulmonary defenses, A549 cells are also known to produce components of surfactant, some of which play a role as host defense molecules in the prevention of *Aspergillus* infection [19–22].

To our knowledge, the present study represents a novel use of galactomannan, and the results demonstrate that levels of this antigen are inextricably linked to the pathogenesis and the

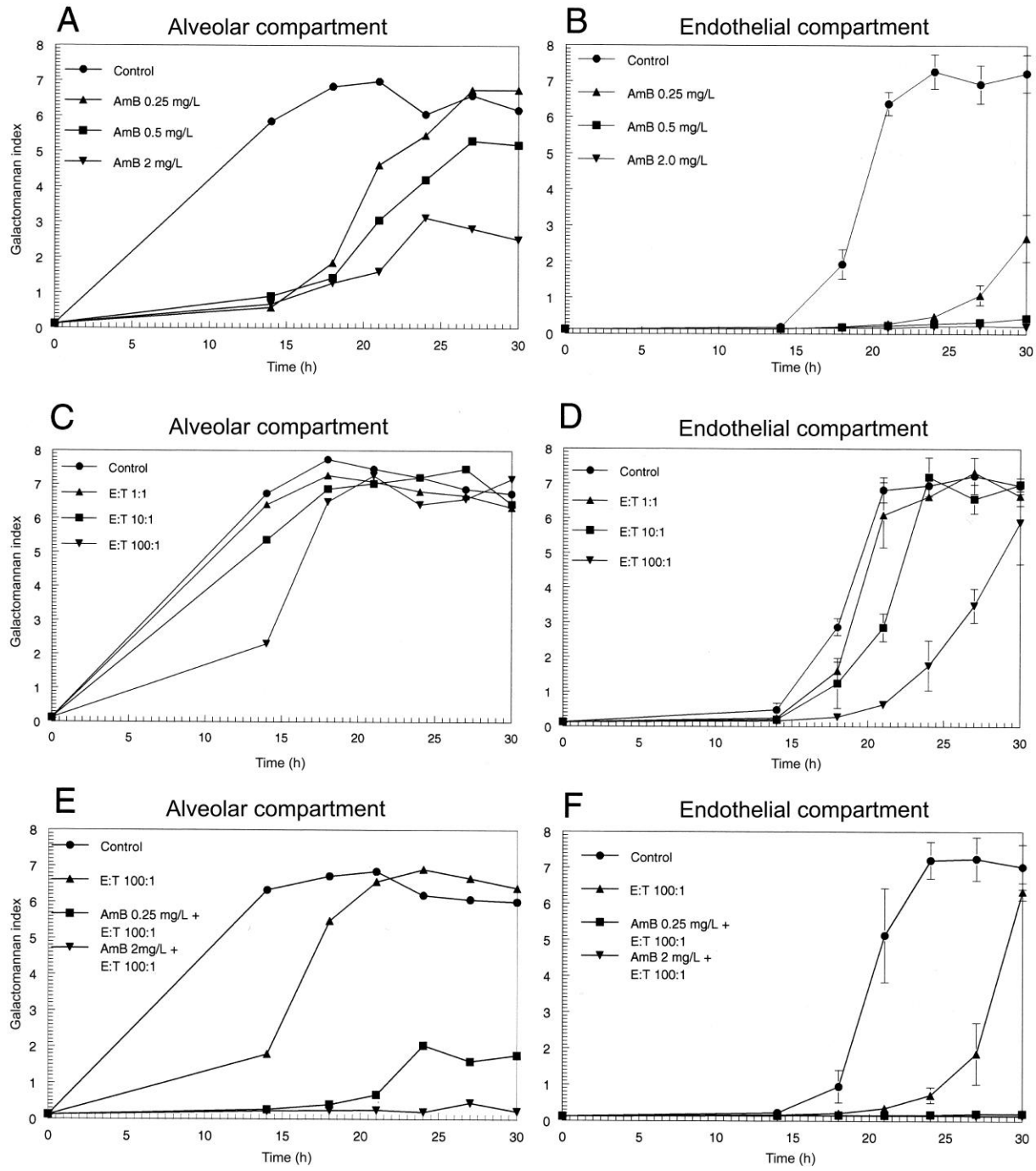


**Figure 6.** Suppression of growth within the alveolar and endothelial compartments when both amphotericin B (AmB) and macrophages are used. *A* and *B,* Effect of 0.25, 0.5, and 2.0 mg/L AmB on the time course of galactomannan in the alveolar and endothelial compartments, respectively. AmB administration did not result in complete suppression of growth when administered alone. *C* and *D,* Effect of macrophages at an effector:target (E:T) ratio of 1:1, 10:1, and 100:1 on the time course of galactomannan in the alveolar and endothelial compartments, respectively. At an E:T ratio of 100:1, there was incomplete suppression of growth. *E* and *F,* Effect of the combination of AmB and macrophages at an E:T ratio of 100:1 on the time profile of galactomannan. An initial concentration of AmB 2.0 mg/L in the presence of macrophages resulted in near-maximal suppression of galactomannan levels in the alveolar and endothelial compartments.

dynamics of invasion of *Aspergillus*. These findings complement data obtained from a variety of clinical and experimental settings, in which galactomannan has been correlated with therapeutic efficacy and outcome [5, 13, 23]. We demonstrated a close temporal relationship between the penetration of the endothelial cell layer and an increase in galactomannan levels, which suggests that galactomannan levels in serum may serve as a crucial marker for the initial breaching of the host by the invading fungus. Furthermore, the present study revealed a discordance in the kinetic profile between BAL fluid and serum, which suggests that galactomannan does not traverse the alveolar-capillary barrier and that, for diagnostic and therapeutic purposes, the airways and vasculature should be viewed as distinct compartments.

Previous studies have suggested that the peak concentration:MIC ratio best links drug exposure with outcome [24, 25]. In the present study, however, only a single dose of drug was administered; in this circumstance, there is complete colinearity between peak concentration:MIC and AUC:MIC. For the purposes of computational tractability, we chose to use AUC:MIC as the dynamically linked variable. The mathematical model suggested that an AUC:MIC ratio of 22.10 resulted in suppression of fungal growth in both the alveolar and endothelial compartments. The Monte Carlo simulations enabled this finding to be placed in a clinical context. A dose of 0.3 mg/kg is unlikely to produce sufficient drug exposure for the treatment of IPA—only 5.5% of patients are predicted to achieve adequate drug exposure. By contrast, a progressively higher proportion of simulated patients receiving doses $\geqslant$0.6 mg/kg are predicted to achieve the drug-exposure target. The findings from the model are potentially most representative of empirical or preemptive antifungal therapy in humans. Importantly, however, the target used in the simulations makes no consideration for a multitude of additional factors that may also affect the outcome of patients with IPA treated with amphotericin B; these include issues pertaining to drug-related toxicity [26–28], suboptimal penetration of drug to the infection site, underlying host disease, the timing of therapeutic intervention, and the total duration of therapy. As a consequence, the calculated rates of target attainment associated with doses of 0.6–1.0 mg/kg do not imply that a favorable clinical outcome can also be expected in a similar proportion of patients with IPA.

Despite these limitations, the present in vitro model provides clinically relevant insights into the biological characteristics, diagnosis, and treatment of early IPA. The model highlights the importance of early therapeutic intervention in securing a favorable outcome and is therefore consistent with the findings of earlier clinical studies [29, 30]. Invasion across the alveolar capillary barrier occurs within the initial 24 h after infection, and assiduous monitoring of biomarkers may detect this breach. Innate immunological effectors are required to procure a favorable therapeutic outcome in IPA, which lends support to strategies to reconstitute or augment host defenses as a means of optimizing the therapeutic outcome [31–33]. This in vitro model serves as a paradigm by which questions pertaining to the pathogenesis, detection, and treatment of other fungal pathogens and nonfungal pulmonary pathogens can be addressed.


## Acknowledgments

We thank Professor Margo Moore (Simon Fraser University, Burnaby, British Columbia, Canada) for supplying us with the *Aspergillus fumigatus* transformant, David Perlin for his helpful comments, and Alan Hoofring for the illustrations.


## APPENDIX

The experimental data from all experiments was comodeled using the following 5 simultaneous inhomogeneous differential equations to obtain estimates for means, medians, and dispersions of the 18 model parameters describing the experimental system:

$$\frac{dX(1)}{dt} = B(1) - k_{12} \times X(1) + k_{21} \times X(2) \ , \tag{1}$$

$$\frac{dX(2)}{dt} = k_{12} \times X(1) - k_{23} \times X(2) - k_{21} \times X(2) \ , \tag{2}$$

$$\frac{dX(3)}{dt} = k_{23} \times X(2) \ , \tag{3}$$

$$\frac{dX(4)}{dt} = Kgmax_{e} \times \left[1 - \frac{X(4)}{POPMAX}\right] \times X(4) \tag{4a}$$

$$\times \left\{1 - \left[\frac{(AmB)^{H_e}}{C50_{e}^{He} + (AmB)^{H_e}}\right]\right\} \tag{4b}$$

$$-WBCkillmax \times \left[\frac{X(4)}{WBCkill50_{e} + X(4)}\right] \times R(1) \times X(4) \ , \tag{4c}$$

$$\frac{dX(5)}{dt} = Kgmax \times \left[1 - \frac{X(5)}{POPMAX}\right] \times X(5) \qquad (5a)$$

$$\times \left\{1 - \left[\frac{(AmB)^{H_a}}{C50_a^{Ha} + (AmB)^{H_a}}\right]\right\} \qquad (5b)$$

$$-WBCkillmax \times \left[\frac{X(5)}{WBCkill50_a + X(5)}\right] \times R(2) \times X(5) \ . \qquad (5c)$$

Equations (1), (2), and (3) describe the pharmacokinetics of amphotericin B. Compartments 1, 2, and 3 indicate the endothelial, cellular, and alveolar compartments, respectively. $X(1)$, $X(2)$, and $X(3)$ indicate the amount of amphotericin B (in milligrams) in the respective compartments. The drug was administered as a time-delineated zero-order input into the endothelial compartment, represented by $B(1)$. The volume of the endothelial and alveolar compartments was defined in the output equations (not shown); $k$ represents the various first-order intercompartmental rate constants. The system is closed (i.e., there is no clearance of drug).

Equations (4) and (5) describe the rate of change of galactomannan in the endothelial (compartment 4) and alveolar (compartment 5) compartments, respectively. $X(4)$ and $X(5)$ represent the amount of galactomannan in the endothelial and alveolar compartments. The subscript *e* in equation (4) denotes "endothelial," and the subscript *a* in equation (5) denotes "alveolar." The terms (4a) and (5a) describe the capacity-limited growth of *Aspergillus* (measured in terms of the galactomannan index) in the respective compartments. Growth begins from an initial value (i.e., the galactomannan value at time 0)—the initial condition in the alveolar and endothelial compartments were identified as part of the model-fitting process. *Kgmax* is the constant that describes the maximum rate of growth of *Aspergillus,* and *POPMAX* is the maximum theoretically achievable galactomannan value. As the growth approaches *POPMAX,* it slows and approaches zero. Note that *POPMAX* assumes the same value in both the endothelial and alveolar compartments. The second term in equations (4) and (5) (terms [4b] and [5b], respectively), describes the effect of amphotericin B on the growth of *Aspergillus.* Progressively higher concentrations of amphotericin B lead to a slowing of growth. $C50_e$ and $C50_a$ are the concentrations of amphotericin B at which the effect of drug on the growth of *Aspergillus* is half-maximal in the endothelial and alveolar compartments, respectively. $H_e$ and $H_a$ represent the respective slope functions. The final terms in equations (4) and (5) ([4c] and [5c]) describe the killing effect induced by macrophages. $WBCkillmax_e$ and $WBCkillmax_a$ are the maximum rate of killing in the endothelial and alveolar compartments, respectively, whereas $WBCkill50_e$ and $WBCkill50_a$ represent the galactomannan values at which killing is half-maximal. Macrophages from the various E:T ratios used in the study were allowed to affect the rate of growth in the endothelial and alveolar compartments via the input functions $R(1)$ and $R(2)$.

## References


1. Herbrecht R, Denning DW, Patterson TF, et al. Voriconazole versus amphotericin B for primary therapy of invasive aspergillosis. N Engl J Med **2002**; 347:408–15.
2. Denning DW. Invasive aspergillosis. Clin Infect Dis **1998**; 26:781–803.
3. Patterson TF, Kirkpatrick WR, White M, et al. Invasive aspergillosis: disease spectrum, treatment practices, and outcomes. I3 *Aspergillus* Study Group. Medicine (Baltimore) **2000**; 79:250–60.
4. Pfeiffer CD, Fine JP, Safdar N. Diagnosis of invasive aspergillosis using a galactomannan assay: a meta-analysis. Clin Infect Dis **2006**; 42:1417–27.
5. Hope WW, Walsh TJ, Denning DW. Laboratory diagnosis of invasive aspergillosis. Lancet Infect Dis **2005**; 5:609–22.
6. Andes D. In vivo pharmacodynamics of antifungal drugs in treatment of candidiasis. Antimicrob Agents Chemother **2003**; 47:1179–86.
7. Andes D. Clinical pharmacodynamics of antifungals. Infect Dis Clin North Am **2003**; 17:635–49.
8. Bermudez LE, Sangari FJ, Kolonoski P, Petrofsky M, Goodman J. The efficiency of the translocation of *Mycobacterium tuberculosis* across a bilayer of epithelial and endothelial cells as a model of the alveolar wall is a consequence of transport within mononuclear phagocytes and invasion of alveolar epithelial cells. Infect Immun **2002**; 70:140–6.
9. Wasylnka JA, Moore MM. *Aspergillus fumigatus* conidia survive and germinate in acidic organelles of A549 epithelial cells. J Cell Sci **2003**; 116:1579–87.
10. Wasylnka JA, Moore MM. Uptake of *Aspergillus fumigatus* conidia by phagocytic and nonphagocytic cells in vitro: quantitation using strains expressing green fluorescent protein. Infect Immun **2002**; 70:3156–63.
11. Clinical and Laboratory Standards Institute (CLSI). Reference method for broth dilution antifungal susceptibility testing of filamentous fungi: approved standard M38-A. Wayne, PA: CLSI, **2002**.
12. O'Sullivan CE, Kasai M, Francesconi A, et al. Development and validation of a quantitative real-time PCR assay using fluorescence resonance energy transfer technology for detection of *Aspergillus fumigatus* in experimental invasive pulmonary aspergillosis. J Clin Microbiol **2003**; 41:5676–82.
13. Petraitiene R, Petraitis V, Groll AH, et al. Antifungal activity and pharmacokinetics of posaconazole (SCH 56592) in treatment and prevention of experimental invasive pulmonary aspergillosis: correlation with galactomannan antigenemia. Antimicrob Agents Chemother **2001**; 45: 857–69.
14. Groll AH, Mickiene D, Petraitis V, et al. Comparative drug disposition, urinary pharmacokinetics and renal effects of multilamellar liposomal nystatin and amphotericin B deoxycholate in rabbits. Antimicrob Agents Chemother **2003**; 47:3917–25.
15. Francis P, Lee JW, Hoffman A, et al. Efficacy of unilamellar liposomal amphotericin B in treatment of pulmonary aspergillosis in persistently granulocytopenic rabbits: the potential role of bronchoalveolar D-mannitol and serum galactomannan as markers of infection. J Infect Dis **1994**; 169:356–68.
16. Leary R, Jelliffe R, Schumitzky A, van Guilder M. An adaptive grid, non-parametric approach to pharmacokinetic and dynamic (PK/PD) models. In: Computer−based medical systems, 2001: proceedings of the Fourteenth IEEE Computer Society. Bethesda, MD: Institute of Electrical and Electronics Engineers, **2001**:389–94.
17. Nath CE, McLachlan AJ, Shaw PJ, Gunning R, Earl JW. Population pharmacokinetics of amphotericin B in children with malignant diseases. Br J Clin Pharmacol **2001**; 52:671–80.

18. Birkness KA, Deslauriers M, Bartlett JH, White EH, King CH, Quinn FD. An in vitro tissue culture bilayer model to examine early events in *Mycobacterium tuberculosis* infection. Infect Immun **1999**; 67:653–8.
19. Lieber M, Smith B, Szakal A, Nelson-Rees W, Todaro G. A continuous tumor-cell line from a human lung carcinoma with properties of type II alveolar epithelial cells. Int J Cancer **1976**; 17:62–70.
20. Madan T, Eggleton P, Kishore U, et al. Binding of pulmonary surfactant proteins A and D to *Aspergillus fumigatus* conidia enhances phagocytosis and killing by human neutrophils and alveolar macrophages. Infect Immun **1997**; 65:3171–9.
21. Madan T, Kaur S, Saxena S, et al. Role of collectins in innate immunity against aspergillosis. Med Mycol **2005**; 43(Suppl 1):S155–63.
22. Madan T, Kishore U, Singh M, et al. Protective role of lung surfactant protein D in a murine model of invasive pulmonary aspergillosis. Infect Immun **2001**; 69:2728–31.
23. Boutboul F, Alberti C, Leblanc T, et al. Invasive aspergillosis in allogeneic stem cell transplant recipients: increasing antigenemia is associated with progressive disease. Clin Infect Dis **2002**; 34:939–43.
24. Andes D, Stamsted T, Conklin R. Pharmacodynamics of amphotericin B in a neutropenic-mouse disseminated-candidiasis model. Antimicrob Agents Chemother **2001**; 45:922–6.
25. Wiederhold NP, Tam VH, Chi J, Prince RA, Kontoyiannis DP, Lewis RE. Pharmacodynamic activity of amphotericin B deoxycholate is associated with peak plasma concentrations in a neutropenic murine model of invasive pulmonary aspergillosis. Antimicrob Agents Chemother **2006**; 50:469–73.
26. Bates DW, Su L, Yu DT, et al. Mortality and costs of acute renal failure associated with amphotericin B therapy. Clin Infect Dis **2001**; 32:686–93.
27. Wingard JR, Kubilis P, Lee L, et al. Clinical significance of nephrotoxicity in patients treated with amphotericin B for suspected or proven aspergillosis. Clin Infect Dis **1999**; 29:1402–7.
28. Perfect JR, Lindsay MH, Drew RH. Adverse drug reactions to systemic antifungals. Prevention and management. Drug Saf **1992**; 7:323–63.
29. Aisner J, Wiernik PH, Schimpff SC. Treatment of invasive aspergillosis: relation of early diagnosis and treatment to response. Ann Intern Med **1977**; 86:539–43.
30. von Eiff M, Roos N, Schulten R, Hesse M, Zuhlsdorf M, van de Loo J. Pulmonary aspergillosis: early diagnosis improves survival. Respiration **1995**; 62:341–7.
31. Dignani MC, Anaissie EJ, Hester JP, et al. Treatment of neutropenia-related fungal infections with granulocyte colony-stimulating factor-elicited white blood cell transfusions: a pilot study. Leukemia **1997**; 11:1621–30.
32. Rodriguez-Adrian LJ, Grazziutti ML, Rex JH, Anaissie EJ. The potential role of cytokine therapy for fungal infections in patients with cancer: is recovery from neutropenia all that is needed? Clin Infect Dis **1998**;26: 1270–8.
33. Segal BH, Kwon-Chung J, Walsh TJ, et al. Immunotherapy for fungal infections. Clin Infect Dis **2006**; 42:507–15.